



저작자표시-비영리-변경금지 2.0 대한민국

이용자는 아래의 조건을 따르는 경우에 한하여 자유롭게

- 이 저작물을 복제, 배포, 전송, 전시, 공연 및 방송할 수 있습니다.

다음과 같은 조건을 따라야 합니다:



저작자표시. 귀하는 원저작자를 표시하여야 합니다.



비영리. 귀하는 이 저작물을 영리 목적으로 이용할 수 없습니다.



변경금지. 귀하는 이 저작물을 개작, 변형 또는 가공할 수 없습니다.

- 귀하는, 이 저작물의 재이용이나 배포의 경우, 이 저작물에 적용된 이용허락조건을 명확하게 나타내어야 합니다.
- 저작권자로부터 별도의 허가를 받으면 이러한 조건들은 적용되지 않습니다.

저작권법에 따른 이용자의 권리는 위의 내용에 의하여 영향을 받지 않습니다.

이것은 [이용허락규약\(Legal Code\)](#)을 이해하기 쉽게 요약한 것입니다.

[Disclaimer](#)

의학박사 학위논문

간세포암에서
sorafenib 과 hexokinase-II
억제제인 3-Bromopyruvate
병합요법의 상승적 항암효과

2019 년 7 월

서울대학교 대학원

의학과 내과학

유 정 주

A thesis of the Degree of Doctor of Philosophy

Hexokinase–II inhibition
synergistically augments the
anti–tumor efficacy of sorafenib
in hepatocellular carcinoma

July 2019

The Department of Internal Medicine

Seoul National University

College of Medicine

Jeong–Ju Yoo

Hexokinase-II inhibition
synergistically augments the anti-
tumor efficacy of sorafenib in
hepatocellular carcinoma

지도교수 윤 정 환

이 논문을 내과학 박사학위논문으로 제출함

2019년 7월

서울대학교 대학원
의학과 내과학
유 정 주

유정주의 박사 학위논문을 인준함
2019년 7월

위원장	<u>김혜령</u>	(인)
부위원장	<u>윤정환</u>	(인)
위원	<u>김용태</u>	(인)
위원	<u>서경석</u>	(인)
위원	<u>이준성</u>	(인)

Hexokinase–II inhibition synergistically
augments the anti–tumor efficacy of
sorafenib in hepatocellular carcinoma

by

Jeong–Ju Yoo, M.D.

A Thesis Submitted to the Department of Internal
Medicine in Partial Fulfillment of the requirements for the
Degree of Doctor of Philosophy in Medicine at the Seoul
National University College of Medicine

July, 2019

Approved by thesis committee:

Professor	<u>Haeryoung Kim</u>	Chairman
Professor	<u>Jung–Hwan Yoon</u>	Vice Chairman
Professor	<u>Yong–Tae Kim</u>	
Professor	<u>Kyung–Suk Suh</u>	
Professor	<u>June–Sung Lee</u>	

ABSTRACT

Introduction: This study aimed to examine whether inhibition of hexokinase (HK)–II activity enhances the efficacy of sorafenib in *in vivo* models of hepatocellular carcinoma (HCC), and to evaluate the prognostic implication of HK–II expression in patients with HCC.

Methods: 3-bromopyruvate (3-BP) was used as a HK–II inhibitor to target HK–II. The human HCC cell line was tested as both subcutaneous and orthotopic tumor xenograft models in BALB/c nu/nu mice. The prognostic role of HK–II was evaluated from HCC patients in The Cancer Genome Atlas (TCGA) database and validated in patients treated with sorafenib.

Results: Quantitative real-time polymerase chain reaction, western blot analysis, and immunohistochemical staining revealed that HK–II expression is upregulated in the presence of sorafenib. Further analysis of the endoplasmic reticulum–stress network model in two different murine HCC models showed that the introduction of additional stress by 3-BP treatment synergistically increased the *in vivo/vitro* efficacy of

sorafenib. HCC patients with increased HK-II expression in the TCGA database showed poor overall survival, and also showed similar results in patient with sorafenib treatment.

Conclusions: These results suggest that HK-II is a promising therapeutic target to enhance the efficacy of sorafenib and that HK-II expression might be a prognostic factor in patients with HCC.

Keywords: hepatocellular carcinoma, sorafenib, hexokinase inhibitor, bromopyruvate

Student number: 2015-30556

CONTENTS

Abstract	i
Contents	iii
List of tables and figures	iv
List of abbreviations.....	vii
Introduction	1
Material and Methods	3
Results	16
Discussion	43
References	48
Abstract in Korean.....	55

LIST OF TABLES AND FIGURES

Table 1. Primer sequences for quantitative real-time polymerase chain reaction.	6
Table 2. Development of the tumor growth kinetics model by backward elimination from the full model	26
Table 3. Baseline characteristics of study population in TCGA database	34
Table 4. Baseline characteristics of study population.....	38
Table 5. Factors identified on univariate and multivariate analyses that affect time to progression in HCC patients treated with sorafenib.....	41
Table 6. Factors identified on univariate and multivariate analyses that affect overall survival in HCC patients treated with sorafenib.....	42
Figure 1. Effect of sorafenib and 3-BP on human HCC cell growth.....	16

Figure 2. Enhanced glycolysis after sorafenib could be targeted by a hexokinase II inhibitor.....	18
Figure 3. Sorafenib resulted in upregulation of hexokinase-II expression in HCC tumors.	19
Figure 4. Hypoxia inhibited the effect of sorafenib on proliferation of human HCC cells.....	20
Figure 5. Inhibition of HK-II by 3-BP reverses increased ER stress and sorafenib resistance.....	22
Figure 6. 3-BP improves the anti-tumor activity of sorafenib against subcutaneous HCC tumors.....	25
Figure 7. 3-BP improves the anti-tumor efficacy of sorafenib against orthotopic HCC tumors: bioluminescent imaging and microscopy imaging.....	30
Figure 8. 3-BP improves the anti-tumor efficacy of sorafenib against orthotopic HCC tumors: total flux and immunohistochemistry.....	31

Figure 9. Upregulated intratumoral HK-II predicts poor survival in TCGA database	33
Figure 10. Immunohistochemical analysis for HK-II protein expression in HCC patients cohort	37
Figure 11. Survival analysis according to the HK-II expression level	40

LIST OF ABBREVIATIONS

HCC	hepatocellular carcinoma
HK-II	hexokinase-II
PVDF	polyvinylidene difluoride
3-BP	3-bromopyruvate
PCR	polymerase chain reaction
eIF2 α	eukaryotic initiation factor 2 α
ROI	regions of interest
TCGA	The Cancer Genome Atlas
OS	overall survival
BCLC	Barcelona clinic liver cancer
mRECIST	modified Response Evaluation Criteria in Solid Tumors
SD	standard deviation
TTP	time to progression
ER	endoplasmic reticulum
AUC	area under the curve
IQR	interquartile range
HR	hazard ratio
CI	confidence interval

INTRODUCTION

Hepatocellular carcinoma (HCC) is one of the leading worldwide causes of cancer-related deaths and is the second most common cancer in men worldwide.¹ Because many patients are still diagnosed at an advanced stage, and there is no effective systemic therapy, the median survival of untreated patients remains poor.² Sorafenib is the only approved systemic therapy for patients with advanced HCC³; however, sorafenib monotherapy confers a modest survival gain compared to placebo.^{4,5} Moreover, the prognostic factors of patients undergoing sorafenib treatment and the mechanisms that mediate sorafenib resistance have not been fully revealed.⁶

Several studies have demonstrated that a variety of mechanisms are involved in sorafenib resistance, which includes increased MAPK14 activity⁷, activation of PI3K/AKT signaling⁸, overexpression of CD44⁹, and enhanced glycolysis.¹⁰⁻¹² Studies on cellular metabolism and glycolysis have provided intriguing information for sorafenib therapy, which has been shown to lead to the inhibition of oxidative phosphorylation and the enhancement of glycolysis in a subset of HCC cell lines.^{10,13} In the glycolytic pathway, hexokinase

(HK)-II catalyzes the first irreversible and rate-limiting step¹⁴, but data on the prognostic role of HK-II activity after sorafenib for patients with HCC are scarce.

The aim of this study was to evaluate if upregulated HK-II expression not only can lead to the reduced efficacy of sorafenib, but also can be a predictor of tumor resistance to sorafenib. In order to investigate whether or not the upregulation of HK-II expression affects the efficacy of sorafenib, the activity of sorafenib in HK-II overexpressing human HCC cell lines in *in vivo* mouse models was analyzed. In addition, the role HK-II expression as a prognostic indicator in sorafenib-treated patients was retrospectively evaluated.

MATERIALS AND METHODS

Cell Lines

The SNU-761 human HCC cell line¹⁶ was maintained in RPMI-1640 medium (WelGene Inc., Seoul, Korea) containing 10% heat-inactivated fetal bovine serum and 1% penicillin/streptomycin at 37°C in a humidified incubator with 5% CO₂. The culture medium was replaced every three days.

A lentivirus was used for the stable transduction of the firefly luciferase-expressing SNU-761 cells. Stock virus was generated in the 293FT cell line, which was co-transfected via Lipofectamine[®] 2000 (Invitrogen, Carlsbad, CA, USA) with the pMSCV/luciferase vector (5 µg), a gag-pol vector (5 µg), and an envelope vector (5 µg). Supernatants were collected at 48 h posttransfection and filtered with 0.45-µm polyvinylidene difluoride (PVDF) filters (Millipore, Billerica, MA, USA). Virus supernatants were tittered and stored at -80 °C until required. For viral transduction of cancer cells, virus containing medium was added to target cells and polybrene (hexadimethrine bromide, 8 µg/mL) or protamine sulfate was also added to the target cells. Luciferase-expressing cancer cells were pooled after puromycin selection.

Chemicals and Reagents

The agent 3-bromopyruvate (3-BP) was obtained from Sigma-Aldrich, Inc. (St. Louis, MO, USA). Sorafenib was purchased from LC laboratories (Woburn, MA, USA).

Lactate Assay

Lactate production was used as a surrogate marker of glycolysis.¹¹ The SNU-761 cells were exposed to vehicle alone (control group), sorafenib alone (8 μ M), 3-BP alone (75 μ M) or both sorafenib (8 μ M) + 3-BP (75 μ M) for 3 h. The levels of extracellular lactate, the end product of glycolysis, were measured by a lactate colorimetric/fluorometric assay (Kit #K607; BioVision, CA, USA).

Reverse Transcription PCR and Quantitative Real-time PCR

The expression of genes induced by ER stress, GADD34 and GADD153, was monitored.^{17,18} Total RNA was extracted with the RNeasy Plus Micro Kit (Qiagen, Venlo, The Netherlands). The cDNA was synthesized with the use of the 1st Strand cDNA Synthesis Kit (Roche Applied Science, Penzberg, Upper Bavaria, Germany). The Applied Biosystems Power SYBR

Green Master Mix System (Life Technologies, Carlsbad, CA, USA) was used for quantitative polymerase chain reaction (PCR). Each sample was analyzed in duplicate. Primer sequences are shown in Table 1. The identities of all PCR products were verified by sequencing.

Table 1. Primer sequences for quantitative real-time polymerase chain reaction

Primer name	Primer sequence
GADD153-for	5'-TGAGCGTATCATGTTAAAGATGAGCG-3'
GADD153-rev	5'-GGTGTGGTGTATGTATGAAGATACACTTCC-3'
GADD34-for	5'-TGATCCGGACCCTGAGACTCC-3'
GADD34-rev	5'-CCCAGACAGCCAGGAAATGG-3'

Immunoblot Assay

Immunoblot assays were performed in the same manner as described in previous studies.^{19,20} Briefly, cells were lysed for 20 min on ice with lysis buffer (50 mM Tris-HCl, pH 7.4; 1% Nonidet P-40; 0.25% sodium deoxycholate; 150 mM NaCl; 1 mM EDTA; 1 mM phenylmethylsulfonyl fluoride; 1 µg/L each of aprotinin, leupeptin, pepstatin; 1 mM Na₃VO₄; 1 mM NaF) and centrifuged at 14,000×g for 10 min at 4°C. Samples were resolved by sodium dodecyl sulfate polyacrylamide gel electrophoresis, transferred to nitrocellulose membranes, exposed to appropriate primary antibodies, and incubated with peroxidase-conjugated secondary antibodies (Biosource International, Camarillo, CA, USA). Bound antibodies were visualized via the use of a chemiluminescent substrate (ECL; Amersham, Arlington Heights, IL, USA) and exposed to Kodak X-OMAT film. The primary antibodies used in this study were as follows: mouse anti-phospho-eukaryotic initiation factor 2α (eIF2α) and anti-actin were obtained from Santa Cruz Biotechnology, Inc. (Santa Cruz, CA, USA); rabbit anti-caspase-9, rabbit anti-caspase-7 and mouse anti-phospho-JNK were obtained from Cell Signaling Technology, Inc.

(Danvers, MA, USA).

Animal Studies

Male BALB/c nu/nu mice were purchased from Orient-Bio (Seongnam, Korea). All animal experiments were approved by the Institutional Animal Care and Use Committee at Seoul National University Hospital (SNUH-IACUC). To establish subcutaneous tumors, 1×10^6 cells of SNU-761 in 40 μL of Matrigel were injected into the left flank of 7-week-old mice. Mice with 150- to 200- mm^3 tumors were randomly assigned to 4 groups (8 mice per group). Tumor volume was measured by calipers every week and calculated by the following formula $V = (\text{length [mm]} \times \text{width [mm]}^2) \times 0.5 [\text{mm}]^3$. Orthotropic tumors were established by injecting 2.5×10^6 cells of luciferase-expressing SNU-761 in 40 μL of PBS under the subcapsular left liver lobe of anesthetized mice after subcostal mini laparotomy. Six days after the procedure, the mice were randomized into the following 4 groups (control, sorafenib, 3-BP, and sorafenib + 3-BP) based on the adequate luciferase signals as measured by IVIS 100 (total flux $>1 \times 10^6$ photon/s/cm²/sr). An IVIS100 imaging system (Caliper Life

Sciences, Hopkinton, MA, USA) was used for the acquisition of bioluminescent images. D-luciferin potassium salt (0.3 mg/mL in saline before use) was used as a substrate for luciferase, and 100 μL of the D-luciferin solution was injected intraperitoneally into the mice. Bioluminescent images were serially acquired until maximum signals were obtained. To quantify emitted light, regions of interest (ROI) were drawn over the regions of the tumors. Total photon flux was expressed as photons per cm^2 per second per steradian ($\text{p}/\text{cm}^2/\text{s}/\text{sr}$). Drugs (1.25 mg/kg/day for sorafenib, 1 mg/kg/day for 3-BP) were injected intraperitoneally every 5 days for 4 weeks.^{19,21} Bioluminescent images were acquired and the weights of mice were also obtained, at baseline, 7, 14, 21, and 28 days after the tumor cells were injected. Specimens of tumor tissue were fixed in 10% formaldehyde and subjected to immunohistochemical staining and TUNEL assay.

Quantitation of apoptosis

TUNEL assay by ApopTag In Situ Apoptosis Detection Kits (Millipore) were performed to assess apoptosis in tumor tissue. Six high-power fields ($\times 400$) with randomly selected were

investigated, and positive TUNEL cells were counted. The percentage of apoptotic cells were calculated by the ratio of apoptotic cells to total cells counted $\times 100$. Minimum 400 cells were counted for each treatment. All procedures involving animals were approved by the Institutional Animal Care and Use Committee at Seoul National University, Republic of Korea and they were consistent with the Guide for the Care and Use of Laboratory Animals.

Immunohistochemical analysis

Anti-Hexokinase II (clone 3D3) and anti-Caspase 3 (clone ab13847) antibodies were purchased from Abcam. Anti-JNK (clone sc-6254) antibody was obtained from Santa Cruz Biotechnology. Immunostaining was done using Ventana Optiview system (Roche Diagnostics, Mannheim, Germany). Slides were scanned by Aperio ScanScope CS2 (Leica Biosystems, Nussloch, Germany) and image files of each core were obtained. PDI immunopositivity was calculated by the Positive Pixel Count Algorithm of the Aperio ImageScope (Leica Biosystems). Two or more cores per case were examined and the highest value was used as a representative

value.

Tumor growth kinetics

To describe the tumor growth kinetics, an exponential model has been selected. Data were analyzed in the same manner as the previous study. The equation used after sorafenib and/or 3-BP administration was as follows: $V = V_0 \times \exp(k \times T)$. V_0 and V are the tumor volumes at baseline and T days later, and k is the growth rate constant related to the tumor doubling time. Data were analyzed with a nonlinear mixed effect modeling (NONMEM) software program (version V, level 1.1, Double Precision), and the first-order conditional estimation method and the PRED routine was used. Exponential random effect models were used to model inter-individual variability for k and V_0 . For example, the baseline tumor volume was modeled as $V_{0i} = V_0 \times \exp(\eta_i)$, where V_0 indicates the typical value for baseline tumor volume for the population and V_{0i} indicates the baseline tumor volume for an individual i . The η_i is a random variable with normal distribution with mean 0 and variance $\omega^2 V_0$. Additionally, the combination of additive and proportional error model represented as $Y_{ij} = \hat{Y}_{ij} \times (1 + \epsilon_{ija}) + \epsilon_{ijp}$ was

used to model residual variability. In this model, Y_{ij} and \hat{Y}_{ij} represent j th observed and predicted tumor volume in individual i , and ϵ_{ija} and ϵ_{ijp} are random variables of normal distribution with mean 0 and variances σ_a^2 and σ_p^2 , for measurement j in individual i .

Human Study

Hexokinase-II mRNA expression levels were retrieved from the The Cancer Genome Atlas (TCGA) RNA sequence database (<http://genome-cancer.ucsc.edu/>). The study included patients who were histopathologically diagnosed with HCC, had not undergone pretreatment, and had complete data on overall survival (OS).²²

Eligibility criteria, treatment regimen and assessment of response to sorafenib in patients with HCC

The eligibility criteria for sorafenib therapy were (1) unresectable HCC according to the Barcelona clinic liver cancer (BCLC) staging classification; (2) age < 80 years; (3) an Eastern Cooperative Group performance status of 0 or 1; (4) Child-Pugh grade A or B; (5) white blood cell count > 3,000

cells/mm³, hemoglobin level > 10 g/dL, platelet count >50,000 cells/mm³; and (6) serum total bilirubin < 3.0 mg/dL, serum transaminases < 200 IU/L and serum creatinine < 1.5 mg/dL. These eligibility criteria were based on the vulnerability to adverse side effects. The diagnosis of HCC was confirmed based on hematoxylin–eosin staining of histopathological specimens in all patients. Sorafenib was given orally at a dose of 400 mg twice daily. Treatment interruptions and up to two dose reductions (first to 400 mg once daily and then to 400 mg every 2 days) were permitted for drug–related adverse effects [the Common Terminology Criteria for Adverse Events (version 3)]. Treatment was continued until the radiologic progression, as defined by the modified Response Evaluation Criteria in Solid Tumors (mRECIST). Assessed by contrast enhanced computed tomography or magnetic resonance imaging every 6–8 weeks, therapeutic response to sorafenib was defined according to the criteria of mRECIST.

Statistical Analysis

All *in vitro* experimental data were obtained from at least 3 independent cell line experiments from a minimum of 3 separate

isolations and are expressed as means \pm standard deviation (SD). The Mann–Whitney U was used to determine differences between groups. For the retrospective patient study, the time to progression (TTP) was calculated from the first day of sorafenib administration to the date of progression. OS was calculated from the date of first administration of sorafenib to the date of death or last contact. Conventional clinical factors at the time of entry into the study and immunopositivity for HK–II were analyzed to identify variables that affected survival as determined by the Kaplan–Meier method and compared by the log–rank test. Stepwise multivariate analysis was performed using the Cox proportional hazards model to identify independent variables that affected survival. Factors found to be significantly related to outcome by univariate analysis were included in the multivariate analysis. For statistical analysis, SPSS version 21.0 for Windows (SPSS, Inc., Chicago, IL, USA) was used. Where $p < 0.05$, it was considered statistically significant.

Institutional Review Board Statement

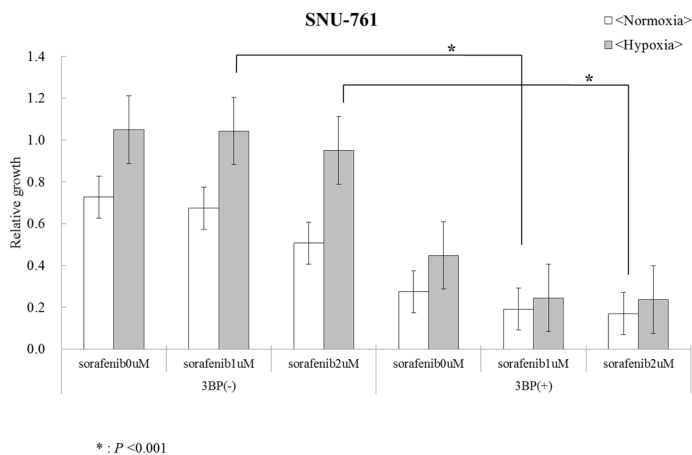
The study protocol was approved by the Institutional Review

Board of the hospital (H-1003-099-314, Seoul National University Hospital Institutional Review Board, 30 April 2010), and also conformed to the ethical guidelines of the World Medical Association Declaration of Helsinki. The biospecimens for this study were provided by the Seoul National University Hospital Human Biobank, a member of the Korea Biobank Network, which is supported by the Ministry of Health and Welfare. All samples derived from the National Biobank of Korea were obtained with informed consent under institutional review board-approved protocols.

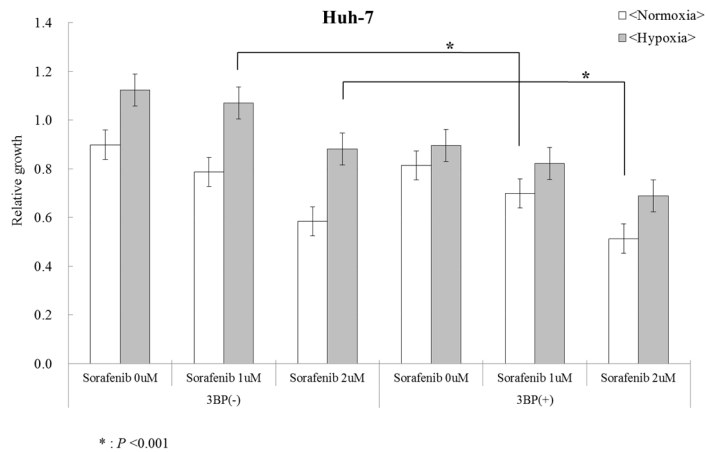
RESULTS

Sorafenib Treatment Leads to Upregulation of Hexokinase-II Expression in Tumor Cell Cultures

Whether 3-BP combined with sorafenib inhibited proliferation of HCC cells *in vitro* was first investigated. For this purpose, human HCC cell lines, SNU-761 (Figure 1A) and Huh-7 (Figure 1B) were cultured in normoxic and hypoxic state. Sorafenib inhibited cellular growth in a dose-dependent manner, and this effect of growth inhibition was amplified when combined with 3-BP, both in normoxic and hypoxic conditions. In short, 3-BP in combination with sorafenib strongly inhibited primary tumor growth.



(A)



(B)

Figure 1. Effect of sorafenib and 3-BP on human HCC cell growth. SNU-761 cells (A), and Huh-7 cells (B) were serum starved for 16 h and treated with sorafenib and/or 3-BP. Cell growth was determined using the MTS assay. Combination of 3-BP with sorafenib effectively inhibited cell growth in hypoxic condition compared with sorafenib alone both SNU-761 and Huh-7 cells. n=3, Student's t-test. * $P < 0.05$

Since the anti-angiogenic effect of sorafenib might induce tumor cells to rely increasingly on glycolysis instead of oxidative phosphorylation, we evaluated culture supernatant lactate levels as a surrogate marker for glycolysis. As shown in Figure 2, the cells receiving sorafenib significantly increased lactate production, which indicated increased glycolysis compared to the control cells under normoxic culture conditions ($p = 0.032$). Next, whether the increased glycolysis after sorafenib was HK-II dependent was evaluated. Increased

glycolysis after sorafenib was reversed by 3-BP, an HK-II inhibitor ($p=0.024$) (Figure 2). Taken together, the results showed that sorafenib resulted in increased glycolysis in an HK-II dependent manner, and HK-II can be targeted by 3-BP.

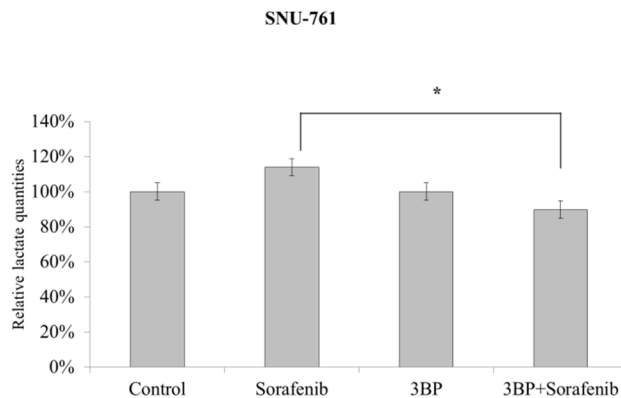


Figure 2. Enhanced glycolysis after sorafenib could be targeted by a hexokinase II inhibitor. SNU-761 cells were exposed to vehicle alone (control group), sorafenib alone (8 μM), 3-BP alone (75 μM) or a co-treatment of sorafenib (8 μM) + 3-BP (75 μM) for 3 hours. Extracellular lactate, the end-product of glycolysis, levels were measured by Lactate Colorimetric/Fluorometric Assay Kit (BioVision, CA, USA). $n=3$, Student's t -test. $*P = 0.048$.

Next, we tested the effect of sorafenib on HK-II expression in a preclinical subcutaneous HCC murine model of SNU-761 tumors. Sorafenib administration was initiated two weeks after injection of SNU-761 cells (when tumors were palpable (50 mm^3)). As shown in Figure 3A, sorafenib caused marginal inhibition of subcutaneous tumors four weeks after the injection

of tumor cells ($p=0.048$). Immunohistochemical analysis showed that HK-II expression was significantly increased in tumors after sorafenib treatment ($p<0.0001$, Figure 3B).

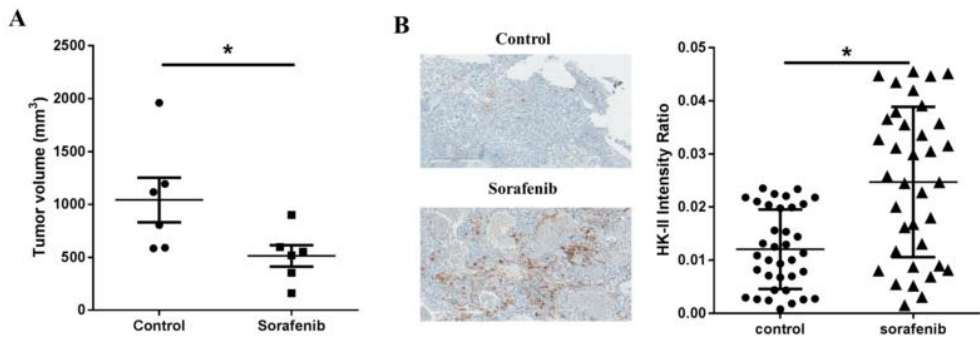


Figure 3. Sorafenib resulted in upregulation of hexokinase-II expression in hepatocellular carcinoma (HCC) tumors. (A) Murine subcutaneous HCC model of SNU-761 tumors. Sorafenib and/or 3-BP were administered two weeks after subcutaneous injection of SNU-761 cells ($n=5$, Mann-Whitney test, $*p=0.043$); (B) hexokinase (HK)-II expression was analyzed by immunohistochemical staining of specimens from each experimental group. The expression of HK-II was significantly lower in the tumors of mice receiving sorafenib + 3-BP than in the tumors of mice receiving sorafenib alone ($n=5$, Mann-Whitney test, $*P < 0.0001$).

Hypoxia Inhibits the Efficacy of Sorafenib Treatment in HCC

The upregulation of HK-II expression associated with sorafenib treatment prompted us to test the relationship between hypoxia and sorafenib, an anti-angiogenic agent, in

more detail. Since hypoxia is reported to induce HK-II expression²³, whether hypoxia inhibited the effect of sorafenib on the proliferation of HCC *in vitro* was investigated. The human HCC cell line SNU-761 was cultured under normoxic and hypoxic conditions in the presence or absence of sorafenib.²⁴ Under the normoxic condition, sorafenib effectively inhibited cellular proliferation ($p = 0.0074$, Figure 4A). By contrast, the hypoxic condition led to significant cellular proliferation compared to the normoxic condition, regardless of the presence of sorafenib (2 μM) (Figure 4B).

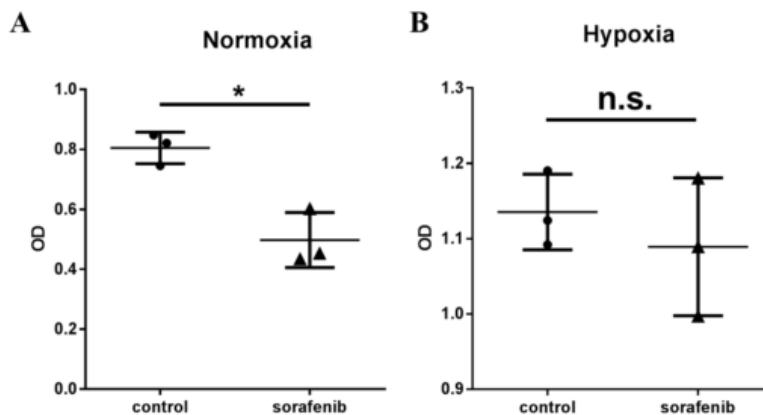


Figure 4. Hypoxia inhibited the effect of sorafenib on proliferation of human HCC cells. SNU-761 cells were serum starved for 16 h and then treated with sorafenib (8 μM) in the presence or absence of 3-BP (75 μM). Cell growth was determined using the MTS assay under (A) normoxic and (B) hypoxic conditions ($n=3$, Mann-Whitney test, $*P < 0.005$).

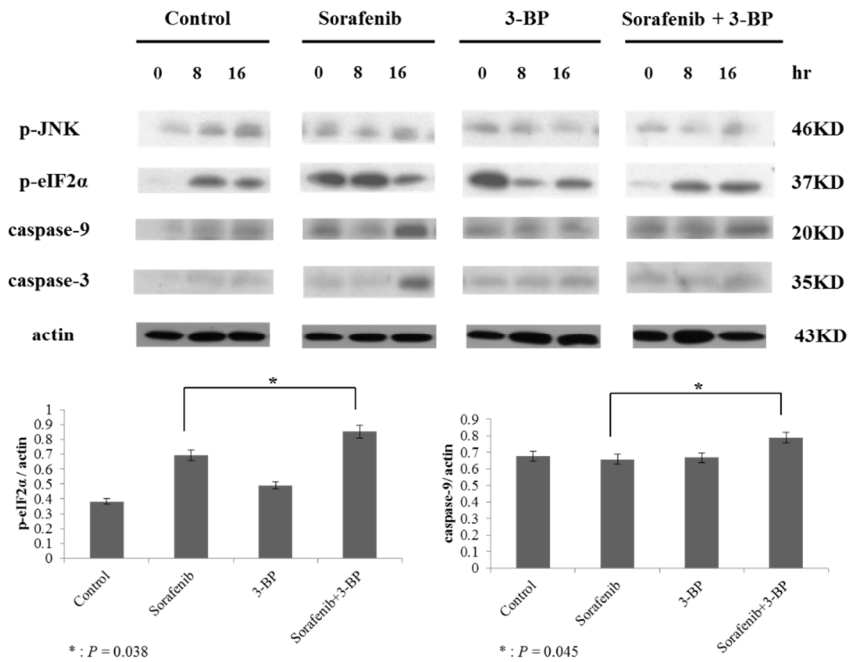
Hexokinase-II Inhibition by 3-BP Rescues Sorafenib Efficacy from Reduced ER Stress

Next, the mechanism of HK-II inhibition to the effect of sorafenib was studied. HK-II, which catalyzes the first step of the major survival pathway induced by hypoxia, was assessed with the use of 3-BP. Because sorafenib exerts its effect on endoplasmic reticulum (ER) stress due to its anti-angiogenic activity, and hypoxia induces HK-II, simultaneous administration of 3-BP and sorafenib might enhance the level of sorafenib-induced apoptosis in HCC cells. When 3-BP was treated with sorafenib, caspase-9 and -3 were more prominent than in the cells treated with just sorafenib alone, indicating that the activation of mitochondrial apoptotic signals was augmented by 3-BP (Figure 5A).

Then, kinase signals that regulate apoptosis was investigated. Pro-apoptotic JNK was more highly activated in cells treated with sorafenib + 3-BP than in cells treated with sorafenib alone (Figure 5A). Because JNK activation might depend on ER stress, the activation of ER stress in cells treated with sorafenib + 3-BP was studied. Indeed, eIF2 α phosphorylation, which reflects activation of ER stress, was prominent in cells

co-treated with sorafenib + 3-BP.

Other ER stress-mediated apoptotic markers, namely, GADD34 and GADD153^{17,18}, were also markedly increased in cells treated with sorafenib + 3-BP, compared to sorafenib alone (Figure 5B). Taken together, these findings suggest that 3-BP might augment ER stress-dependent JNK activation in sorafenib-treated HCC cells, which thus leads to apoptosis of these cells.



(A)

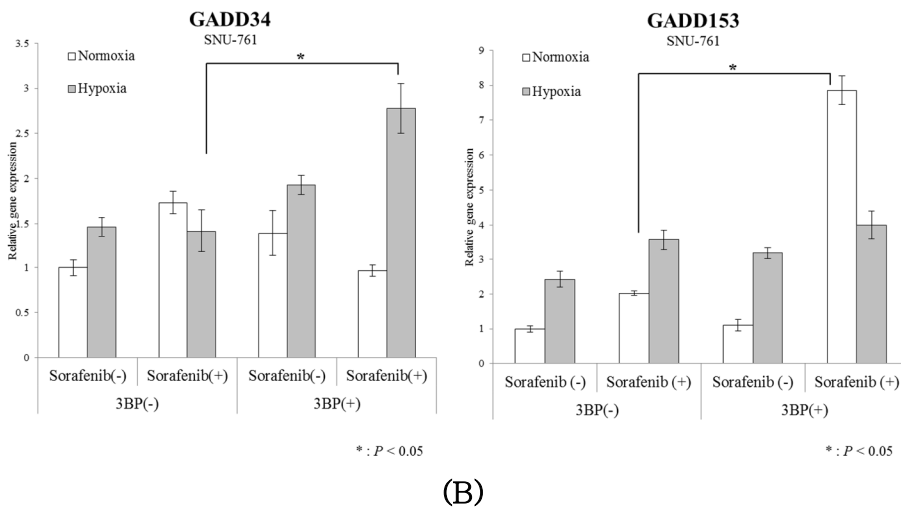


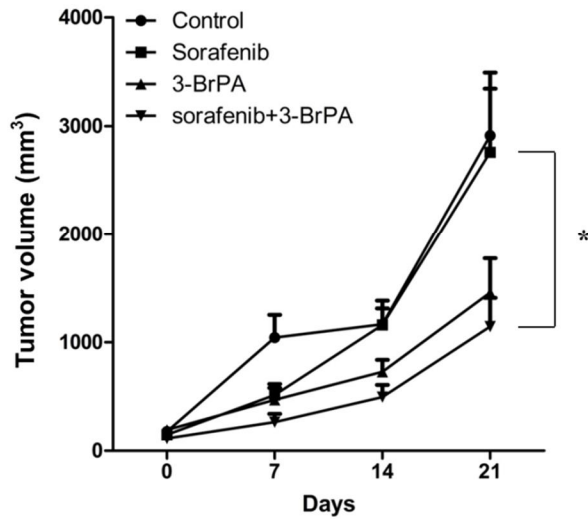
Figure 5. Inhibition of HK-II by 3-BP reverses increased ER stress and sorafenib resistance. The SNU-761 cells were serum starved for 16 h and then treated with sorafenib (8 μ M) in the presence or absence of 3-BP (75 μ M). (A) Equivalent amounts of proteins were immunoblotted using anti-phospho-JNK, anti-phospho-eIF2 α , anti-caspase-9, anti-caspase-3, and anti-actin antibodies. (B) The ER stress markers, GADD34 and GADD153, were evaluated by quantitative real-time PCR. GADD34 and GADD153 were markedly increased in cells treated with sorafenib + 3-BP compared to sorafenib alone, especially in hypoxic and normoxic condition, respectively (n=3, Mann-Whitney test, * $P < 0.05$).

3-BP Augments the Antitumor Efficacy of Sorafenib *In Vivo*

Next, whether or not 3-BP treatment enhances the activity of sorafenib against HCC in BALB/c-nu/nu mice bearing subcutaneous SNU-761 tumors was tested. Compared to the control animals, therapy consisting of sorafenib alone led to only mild suppression of tumor growth (Figure 6). By contrast,

the combination therapy of 3-BP and sorafenib led to the obvious inhibition of tumor growth (Figure 6). After 28 days of treatment, the volumes of the tumors in the groups treated with sorafenib, 3-BP, or combined sorafenib + 3-BP were reduced to 66.5%, 44.6%, and 39.4%, respectively, of the mean tumor size of the untreated control group ($p=0.021$, Figure 6). The synergistic effect was evaluated by NONMEM, based on the assumption that growth of the tumors was exponential. The growth rate constants were significantly larger for the tumors of the mice treated by sorafenib + 3-BP than for the untreated control mice, and mice treated by sorafenib, demonstrating that 3-BP and sorafenib acted synergistically to inhibit tumor growth (Table 2).

Ectopic HCC mice model



* : $P=0.021$

Figure 6. 3-BP improves the anti-tumor activity of sorafenib against subcutaneous HCC tumors. Male BALB/c nu/nu mice were subcutaneously injected with 2.5×10^6 SNU-761 HCC cells. The tumors in HCC xenograft mouse models were blindly measured by calipers. Two weeks after subcutaneous injection, sorafenib and or 3-BP were administered for 21 days ($n=8$, Mann-Whitney test, $*P = 0.032$).

Table 2. Development of the tumor growth kinetics model by backward elimination from the full model

Hypothesis	-2 * log- likelihood	DF	Diff(-2 * log- likelihood)	Chi- square (α =0.05)	p-value	Conclusion
Base model						
K value of each group was identical (k1=k2=k3=k4)	5088.719	2				
Full model						
Was k different according to treatment group?	5055.716	5	32.463	7.81 (df=3)	<0.0001	YES
Backward elimination from the Full model						
Was k different between control group & sorafenib group?	5057.109	4	1.393	3.84 (df=1)	0.2379	NO
Was k different between control group & 3-BP group?	5069.281	4	13.565	3.84 (df=1)	<0.0001	YES
Was k different between control group & sorafenib + 3-BP group?	5066.877	4	11.161	3.84 (df=1)	<0.0001	YES
Was k different between sorafenib group & 3-BP group?	5076.960	4	21.244	3.84 (df=1)	<0.0001	YES
Was k different between sorafenib group & sorafenib + 3-BP group?	5073.222	4	17.506	3.84 (df=1)	<0.0001	YES
Was k different between 3-BP group & sorafenib + 3-BP group?	5055.750	4	0.034	3.84 (df=1)	0.8537	NO

Next, an orthotopic HCC model was established by direct subcapsular injection of SNU-761 cells into the livers of BALB/c-nu/nu livers as a model of HCC patients to study the effect of combined therapy. To visualize tumor growth in the orthotopic HCC mouse model by *in vivo* imaging, an SNU-761-luc cell line was established. The strength of the luciferase signal corresponded to the number of viable cancer cells ($R^2=0.9978$). Consistent with our observations of the subcutaneous tumor model, imaging analysis showed that sorafenib alone or 3-BP alone inhibited progression of the liver tumors. However, the combination treatment of 3-BP + sorafenib showed the strongest anti-tumor effect (Figure 7A). After 28 days of treatment, the bioluminescent signals of the mice receiving sorafenib, 3-BP, or sorafenib + 3-BP were reduced to 85.1%, 36.6% and 19.9%, respectively, of the signals of the controls ($p<0.05$, Figure 8A). Analysis of BLI images was carried out by Living Image 2.50 software (PerkinElmer, Waltham, MA, USA). The bioluminescent signals from tumors were also compared after autopsy (Figure 8B). The upper and middle panels show mouse organs and the sizes of removed livers after abdominal cuts. The bottom panel

shows BLI signals that indicate the presence of injected cells and cellular proliferation. Similar to the results from the subcutaneous model, the combination of 3-BP and sorafenib improved efficacy of sorafenib-based anticancer therapy on HCC. Notably, 3-BP enhanced the therapeutic effect of sorafenib by approximately 40% ($p < 0.05$, Figure 8C). Together, the results obtained from two different HCC murine models, namely, subcutaneous and orthotopic tumors, support the concept that the targeting of HK-II should enhance the efficacy of sorafenib therapy against HCC.

Then, whether or not 3-BP combined with sorafenib enhanced apoptosis in mouse HCC tumors was investigated. The TUNEL staining method was used to quantify apoptosis. The percentage of TUNEL-stained cells was significantly higher in the tumors of mice receiving sorafenib + 3-BP than in the tumors of mice receiving sorafenib alone ($p < 0.05$, Figure 8D). Next, immunohistochemical staining with anti-JNK ($p < 0.05$, Figure 8E) and anti-caspase-3 ($p < 0.05$, Figure 8F) was explored. The intensity of caspase-3 and JNK expression was significantly higher in the tumors of mice receiving sorafenib + 3-BP than in the tumors of mice receiving sorafenib alone.

These findings suggest that 3-BP augmented ER-stress-dependent JNK activation in sorafenib-treated HCC-bearing mice. The microscopy image of each immunohistochemistry is shown in Figure 7B.

livers of recipient male BALB/c nu/nu mice. The establishment and growth of tumors were blindly monitored by bioluminescent imaging (BLI) by the Xenogen IVIS. The intensity of luciferase total flux signals, as measured by BLI represents the rate of proliferation. The mice were followed for up to 28 days. (B) The microscopy image of immunohistochemistry (TUNEL, anti-JNK, and anti-caspase 3).

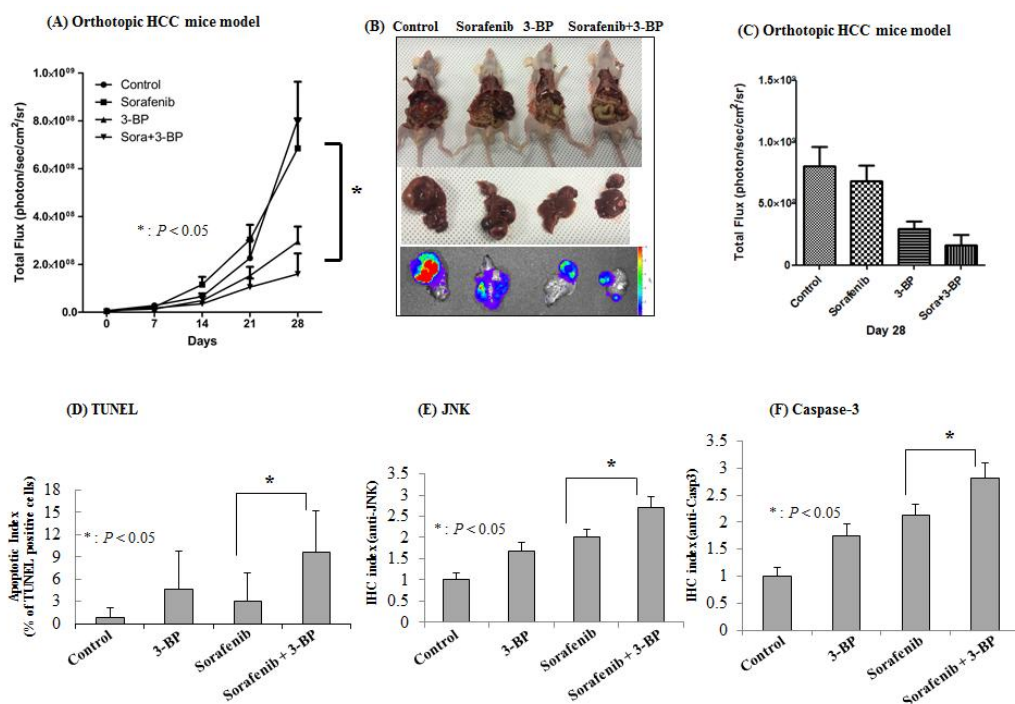


Figure 8. 3-BP improves the anti-tumor efficacy of sorafenib against orthotopic HCC tumors. (A) The bioluminescent image (BLI) signals of the tumor cells from the mice receiving sorafenib, 3-BP, or sorafenib + 3-BP after 28 days of treatment. (B) Representative ex vivo images from autopsy. (C) The BLI signals evaluated immediately after autopsy. (D) The apoptotic index, defined as TUNEL-positive cell percentages of the total number of cells. (E) JNK and (F) caspase-3 immunohistochemical staining of sections of paraffin-embedded HCC specimens.

Prognostic Role of HK-II Expression on Survival of Patients with HCC Patient Survival in the TCGA Database

A total of 224 eligible HCC patients were included in the study. Table 3 summarizes the clinicopathological characteristics of these patients. The median age was 61 years (range 17–85 years). There were 162 (72.3%) patients with N0, 3 (1.3%) patients with N1, and 59 (26.3%) patients with unknown stage disease. Most of the patients (172, 76.8%) did not have distant metastases, 3 (1.3%) had distant metastases, and the other 49 (21.9%) patients had unknown metastatic status. The patients were stratified into two groups according to the degree of HK-II expression, using a cutoff point of 0.2054, which provided the maximum sum of specificity and sensitivity for predicting OS (sensitivity, 57.14%; specificity, 63.39%; area under the curve (AUC), 0.548; 95% CI, 0.457–0.637; $p=0.58$). At the end of the last follow-up, 68 patients had died of the disease, and the proportion of patients who died of the disease showed high HK-II expression levels in their tumors than those were alive. The median OS rates were 56.5 months (interquartile range (IQR) = 12.2–41.4) and 84.7 months (IQR = 13.8–45.6), for the HK-II-high and HK-II-low

patients, respectively (hazard ratio [HR], 1.71; 95% confidence interval [CI], 1.02 to 2.86; $p=0.043$) (Figure 9).

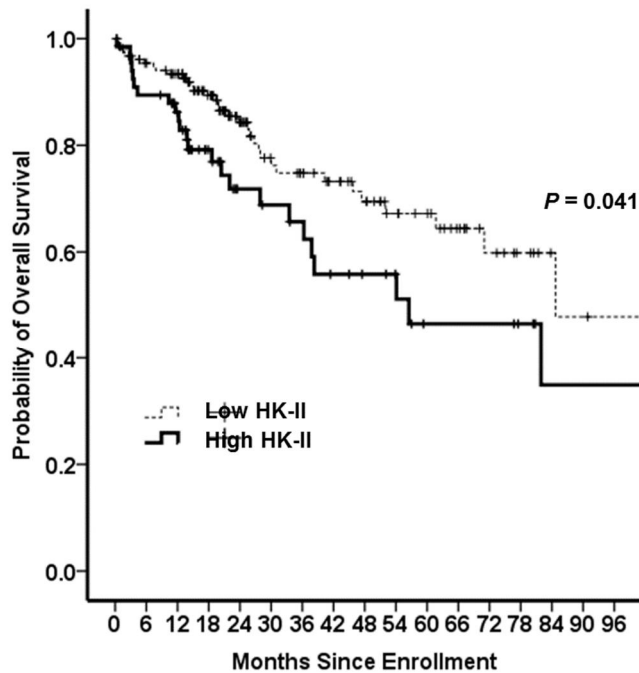


Figure 9. Upregulated intratumoral HK-II predicts poor survival in TCGA database. Kaplan-Meier plots estimated overall survival in patients with HCC based on HK-II expression level. Median survival was 56.5 months and 84.7 months, respectively, for HK-II high and low group, which difference was also statistical significance ($P = 0.041$).

Table 3. Baseline Characteristics of study population in TCGA database

Variable	Total (n=224)	Low HK-II (n=157)	High HK-II (n=67)	<i>P</i>
Age (years) (median (range))	61 (17–85)	61 (20–81)	61 (17–85)	0.884
< 60	98 (43.8%)	68 (43.3%)	30 (44.8%)	
≥ 60	126 (56.2%)	89 (56.7%)	37 (55.2%)	
Gender				0.356
Male	148 (66.1%)	107 (68.2%)	41 (61.2%)	
Female	76 (33.0%)	50 (31.8%)	26 (38.8%)	
Etiology				0.008
HBsAg positive	53 (23.7%)	45 (28.7%)	8 (11.9%)	
Anti-HCV positive	19 (8.5%)	15 (9.6%)	4 (6.0%)	
Alcohol	64 (28.6%)	40 (25.5%)	24 (35.8%)	
NAFLD	7 (3.1%)	7 (4.5%)	0 (0%)	
Hemochromatosis	1 (0.4%)	0 (0%)	1 (1.5%)	
Unknown	80 (35.7%)	50 (31.8%)	30 (44.8%)	
Child-Pugh score (median (range))	5 (5–8)	5 (5–8)	5 (5–8)	0.001
A	145 (64.7%)	115 (73.2%)	30 (44.8%)	
B	16 (7.1%)	10 (6.4%)	6 (9.0%)	
Unknown	63 (28.1%)	32 (20.4%)	31 (46.3%)	
Alpha-fetoprotein (ng/mL)				0.290
< 200	123 (54.9%)	88 (56.1%)	35 (52.2%)	
≥ 200	58 (25.9%)	43 (27.4%)	15 (22.4%)	
Unknown	43 (19.2%)	26 (16.6%)	17 (25.4%)	
T stage				0.083
T1	118 (52.7%)	92 (58.6%)	26 (38.8%)	
T2	54 (24.1%)	32 (20.3%)	22 (32.8%)	
T3	43 (19.2%)	28 (17.9%)	15 (22.4%)	
T4	9 (4.0%)	5 (3.2%)	4 (6.0%)	
N stage				0.063
N0	162 (72.3%)	120 (76.4%)	42 (62.7%)	
N1	3 (1.3%)	1 (0.6%)	2 (3.0%)	
NX	58 (25.9%)	36 (22.9%)	22 (32.8%)	
Unknown	1 (0.4%)	0 (0%)	1 (1.5%)	
M stage				0.983
M0	172 (76.8%)	121 (77.1%)	51 (76.1%)	
M1	3 (1.3%)	2 (1.3%)	1 (1.5%)	
MX	49 (21.9%)	34 (21.7%)	15 (22.4%)	
Resection type				0.677
R0	199 (88.8%)	142 (90.4%)	57 (85.1%)	
R1	10 (4.5%)	6 (3.8%)	4 (6.0%)	

	R2	1 (0.4%)	1 (0.6%)	0 (0%)	
	Rx	10 (4.5%)	6 (3.7%)	4 (6.0%)	
	Unknown	4 (1.8%)	2 (1.3%)	2 (3.0%)	
Grade					0.318
	Grade 1	31 (13.8%)	23 (14.6%)	8 (11.9%)	
	Grade 2	100 (44.6%)	75 (47.8%)	25 (37.3%)	
	Grade 3	85 (37.9%)	53 (33.8%)	32 (47.8%)	
	Grade 4	6 (2.7%)	5 (3.2%)	1 (1.5%)	
	Unknown	2 (0.9%)	1 (0.6%)	1 (1.5%)	

HBsAg, hepatitis B surface antigen; Anti-HCV, antibody against hepatitis C virus; NAFLD, nonalcoholic fatty liver disease.

Elevated High HK-II Expression Predicts a Poor Clinical Outcome in Patients with HCC Who Have Undergone Sorafenib Treatment

Based on our results, HK-II expression and activity were postulated to be correlated with sorafenib resistance. To examine the relationship between HK-II expression and sorafenib sensitivity in patients with HCC, the degree of HK-II immunopositivity in HCC patients who had been treated with sorafenib were analyzed. Immunohistochemical analysis of HK-II protein expression in archived tumor specimens from our HCC patient cohort (n=94) demonstrated that HK-II expression was increased in the tumor tissue of 72 cases (76.6%), whereas 22 cases (23.4%) showed decreased HK-II expression compared to adjacent nonmalignant liver tissue (Table 4, Figure 10).

Hexokinase II expression in Human HCC

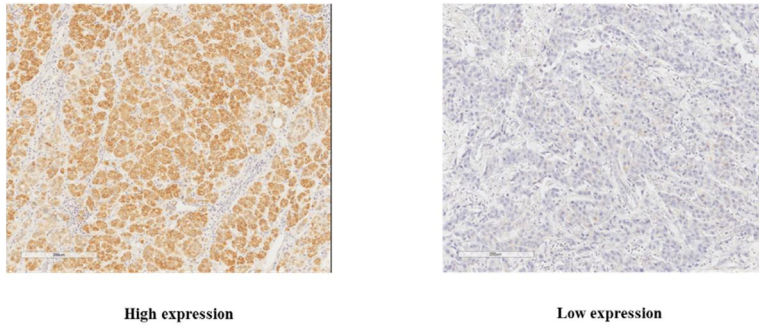


Figure 10. Immunohistochemical analysis for HK-II protein expression in HCC patients cohort. Representative images of high (left panel) and low (right panel) expression of HK-II. x 200.

Table 4. Baseline Characteristics of Study Population

Variable	Total (n=94)	Low HK-II (n=22)	High HK-II (n=72)	<i>P</i>
Age (years) (median (range))	54 (20–76)	58 (35–74)	53 (20–76)	0.126
< 60	61 (64.9%)	11 (50.0%)	50 (69.4%)	
≥ 60	33 (35.1%)	11 (50.0%)	22 (30.6%)	
Gender				0.726
Male	82 (87.2%)	20 (90.9%)	62 (86.1%)	
Female	12 (12.8%)	2 (9.1%)	10 (13.9%)	
Etiology				0.450
HBsAg positive	76 (82.1%)	16 (72.7%)	60 (83.3%)	
Anti-HCV positive	5 (5.3%)	2 (9.1%)	3 (4.2%)	
Alcohol	2 (2.1%)	0 (0%)	2 (2.8%)	
Unknown	11 (10.5%)	4 (18.2%)	7 (9.7%)	
Child-Pugh score (median (range))	5 (5–10)	5 (5–6)	5 (5–10)	0.194
Alpha-fetoprotein (ng/mL)				0.453
< 200	54 (57.5%)	11 (50.0%)	43 (59.7%)	
≥ 200	40 (42.5%)	11 (50.0%)	29 (40.3%)	
Tumor size				0.191
< 5 cm	86 (91.5%)	22 (100.0%)	64 (88.9%)	
≥ 5 cm	8 (8.5%)	0 (0%)	8 (11.1%)	
Tumor number	2.87 ± 3.54	1.50 ± 3.00	3.29 ± 3.59	0.037
Vascular invasion				0.622
No	88 (93.6%)	20 (90.9%)	68 (94.4%)	
Yes	6 (6.4%)	2 (9.1%)	4 (5.6%)	
Edmondson grade (worst)				<0.001
Grade 2	19 (20.2%)	11 (50.0%)	8 (11.1%)	
Grade 3	35 (37.2%)	7 (31.8%)	28 (38.9%)	
Grade 4	40 (42.6%)	4 (18.2%)	36 (50.0%)	

PD, progressive disease; HBsAg, hepatitis B surface antigen;

Anti-HCV, antibody against hepatitis C virus; HK, hexokinase.

The prognostic impact of HK-II expression in HCC tissues of patients treated with sorafenib was examined. As shown in Figure 11A, the Kaplan-Meier curve shows a significant prolongation of the TTP in patients with tumors showing low HK-II expression, compared with the TTP of the patients with high HK-II expression (log-rank, $p=0.048$). High HK-II expression was independently associated with shorter TTP (adjusted HR (aHR) 1.909; 95% CI, 1.086–3.342; $p=0.026$) after adjustment for age (Table 5). Kaplan-Meier analysis also found a significant prolongation of OS in patients with tumors showing low HK-II expression compared with the OS of patients with high HK-II expression (log-rank, $p<0.001$; Figure 11B). High HK-II expression was independently associated with poor OS (aHR 1.882; 95% CI, 1.171–3.190; $p=0.024$; R_squared by Cox & Snell 0.995) after adjustment for Child-Pugh score, tumor number, and lymph node involvement (Table 6).

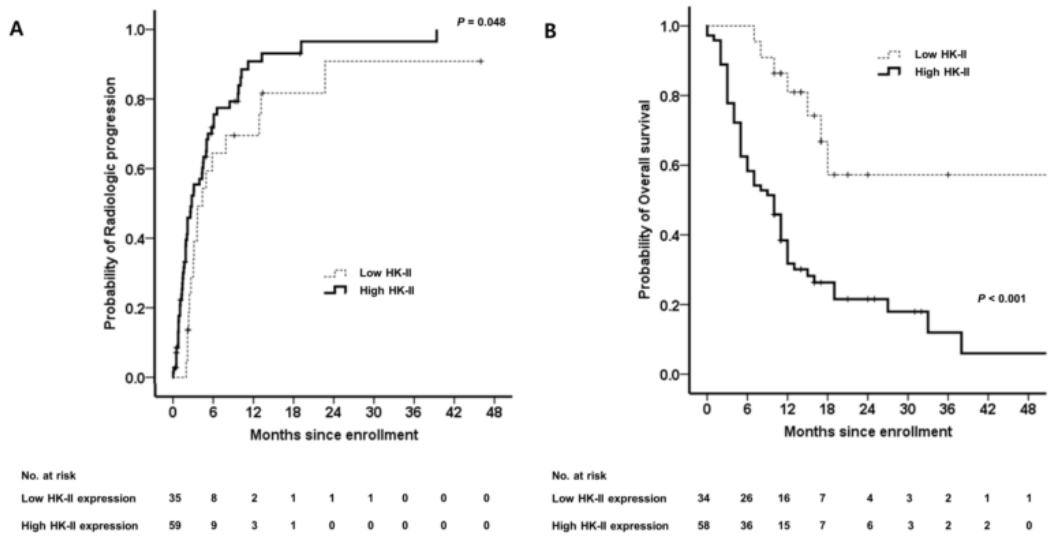


Figure 11. Survival analysis according to the HK-II expression level. (A) Time to progression. (B) Overall survival (OS).

Table 5. Factors identified on univariate and multivariate analyses that affect time to progression in HCC patients treated with sorafenib

Variable	Univariate Analysis		Multivariate Analysis	
	HR	<i>P</i>	Adjusted HR	<i>P</i>
Age (≥ 60 years)	0.559 (0.370–0.889)	0.014	0.592 (0.373–0.937)	0.026
Male	0.908 (0.537–1.572)	0.741		
Etiology				
anti-HCV positive versus HBsAg positive	0.835 (0.261–2.669)	0.761		
Alcohol versus HBsAg positive	1.454 (0.528–4.032)	0.478		
Unknown versus HBsAg positive	0.631 (0.281–1.450)	0.281		
Child-Pugh score	1.072 (0.958–1.170)	0.196		
AFP (ng/mL)				
≥ 200	1.114 (0.731–1.689)	0.625		
Tumor size				
≥ 5 cm	1.208 (0.746–1.699)	0.614		
Tumor number	1.031 (0.972–1.093)	0.412		
Vascular invasion				
Yes	1.493 (0.980–2.245)	0.070		
Lymph node				
Yes	1.579 (0.731–3.460)	0.245		
Metastasis				
Yes	2.521 (1.149–5.490)	0.028		
Edmondson grade (worst)				
Grade 3 versus grade 2	0.735 (0.356–1.512)	0.391		
Grade 4 versus grade 2	1.460 (0.721–3.011)	0.312		
HK-II expression level				
High	1.631 (1.032–2.590)	0.039	1.909 (1.086–3.342)	0.026

Anti-HCV, antibody against hepatitis C virus; HBsAg, hepatitis

B surface antigen; AFP, alpha-fetoprotein; HK, hexokinase.

Table 6. Factors identified on univariate and multivariate analyses that affect overall survival in HCC patients treated with sorafenib

Variable	Univariate Analysis		Multivariate Analysis	
	HR	<i>P</i>	Adjusted HR	<i>P</i>
Age (≥ 60 years)	0.820 (0.481–1.399)	0.470		
Male	0.649 (0.309–1.363)	0.265		
Etiology				
anti-HCV positive versus HBsAg positive	2.049 (0.809–5.139)	0.129		
Alcohol versus HBsAg positive	0.764 (0.149–3.953)	0.750		
Unknown versus HBsAg positive	1.091 (0.123–9.390)	0.941		
Child-Pugh score	2.114 (1.468–3.039)	<0.001	1.967 (1.348–2.871)	<0.001
AFP (ng/mL)				
≥ 200	1.155 (0.724–1.890)	0.545		
Tumor size				
≥ 5 cm	1.345 (0.546–3.512)	0.488		
Tumor number	1.112 (1.051–1.190)	0.001	1.121 (1.033–1.189)	0.002
Vascular invasion				
Yes	1.598 (0.731–3.532)	0.253		
Lymph node				
Yes	2.782 (1.521–5.021)	0.002	2.142 (1.149–3.924)	0.021
Metastasis				
Yes	1.366 (0.621–2.986)	0.481		
Edmondson grade (worst)				
Grade 3 versus grade 2	1.323 (0.482–3.610)	0.571		
Grade 4 versus grade 2	3.564 (1.391–9.221)	0.008		
HK-II expression level				
High	1.721 (1.072–2.912)	0.039	1.882 (1.171–3.190)	0.024

Anti-HCV, antibody against hepatitis C virus; HBsAg, hepatitis

B surface antigen; AFP, alpha-fetoprotein; HK, hexokinase.

DISCUSSION

In this study, we showed that upregulated HK-II expression inhibited sorafenib-induced apoptotic cell death and that this finding could be reversed by 3-BP¹⁵, an HK-II inhibitor. Using various murine HCC models, we also provided evidence of the beneficial effect on sorafenib treatment of added therapy that suppressed HK-II expression. Moreover, we showed that upregulated HK-II expression predicted poor outcomes in patients with HCC who had undergone sorafenib treatment. These findings have important implications for considering sorafenib-based therapy for patients with HCC.

The main finding of this study is the augmented *in vitro* and *in vivo* (HCC animal model) anti-tumor effect provided by 3-BP + sorafenib. This synergistic effect was attributed to the following two mechanisms: (i) the inhibition of aerobic glycolysis, which is enhanced after sorafenib exposure, resulting in energy depletion and apoptosis; and (ii) the promotion of ER stress due to sorafenib, also resulting in augmented apoptosis. Furthermore, the upregulation of HK-II expression in HCC tissue predicted poor survival of patients from TCGA database. We also found that HK-II expression in

the tumors of HCC patients predicted resistance to sorafenib.

Although sorafenib is the only approved systemic chemotherapy for HCC, it has only shown modest results for OS.⁴ Due to genetic diversity, HCC often shows primary resistance to sorafenib.²⁵ Hepatocellular carcinoma also frequently shows secondary resistance associated with sorafenib administration, because of the activation of compensatory pathways, such as the PI3K/Akt and JAK-STAT pathways, EMT, and tumor hypoxia.²⁶ We previously reported that hypoxia induced HK-II expression in HCC cells.¹⁴ In contrast to normal cells, which mostly rely on mitochondrial oxidative phosphorylation to generate energy, most cancer cells rely on aerobic glycolysis, which is known as the ‘Warburg Effect’.²⁷ Indeed, many HCC cell lines are known to rely mainly on aerobic glycolysis for generation of adenosine triphosphate (ATP), in an HK-II-dependent manner.²⁸

Inhibitors of aerobic glycolysis via the Warburg Effect have been reported to be effective, and some of the inhibitors are under clinical study.²⁹ When aerobic glycolysis was blocked, apoptosis was induced mainly by the decreased levels of ATP in cancer cells.¹⁰ Our study also showed that the HK-II

inhibitor, 3-BP, which inhibits glycolysis, is effective, which was demonstrated by a lactate assay. Apoptosis was likely induced by the markedly increased depletion of ATP that was associated with the use of the combination therapy of sorafenib + 3-BP. Indeed, sorafenib, unlike other multikinase inhibitors, has been reported to decrease ATP levels.¹⁰ However, the effect of 3-BP might also be explained by its interactions with the binding sites of other enzymes with anti-kinase activity, but these phenomena still need further research.¹⁰

Increased ER stress is one of the recently observed mechanisms of the antitumor actions of sorafenib. Previous studies have suggested that sorafenib increases ER stress, which leads to caspase-3 induced cell death.¹⁸ Hexokinase-II inhibitors also show activity associated with ER stress. We have previously verified that 3-BP, a type of HK-II inhibitor, increases ER stress, which has also been documented by other investigators.^{19,30,31} The agent 3-BP was first studied as an anti-cancer agent more than a decade ago at Johns Hopkins.³² We previously reported that 3-BP effectively inhibited the *in vitro* and *in vivo* growth of HCC by causing the dissociation of HK-II from the permeability transition pore complex (PTPC),

which activates mitochondrial apoptotic signals.³³ Unlike normal liver tissue, human HCC cells tend to overexpress HK-II, and HK-II overexpression becomes more prominent in a hypoxic environment (*e.g.*, advanced infiltrative hypovascular HCC or after sorafenib administration).¹⁴ Therefore, 3-BP treatment might prove to be a very selective anticancer therapy, because HK-II is maximally expressed in HCC cells and minimally expressed in normal liver tissue.³³ The efficacy of 3-BP as a therapeutic agent was proven by several animal studies, including our previous investigations.³³⁻³⁵

In our patient cohort, HK-II expression was significantly correlated with OS and TTP in patients who had undergone sorafenib treatment. However, we could not find an association between HK-II expression and different stage or tumor grade. Additional studies of other patient cohorts are needed to verify our findings. The relationship between other known resistance factors such as HIF-1 α and VEGFR, and OS and TTP should also be investigated.^{36,37} In addition, a patient-derived xenograft model might be useful to confirm the efficacy of sorafenib combined with an HK-II inhibitor as treatment for HCC.

In conclusion, HK-II is a useful therapeutic target that can lead to enhancement of the efficacy of sorafenib treatment. HK-II expression might also be useful as a marker that predicts sensitivity to sorafenib and clinical outcomes.

REFERENCES

1. El-Serag HB, Kanwal F. Epidemiology of hepatocellular carcinoma in the United States: where are we? Where do we go? *Hepatology* 2014;60:1767–75.
2. Giannini EG, Farinati F, Ciccarese F, et al. Prognosis of untreated hepatocellular carcinoma. *Hepatology* 2015;61:184–90.
3. Yu SJ. A concise review of updated guidelines regarding the management of hepatocellular carcinoma around the world: 2010–2016. *Clin Mol Hepatol* 2016;22:7–17.
4. Llovet JM, Ricci S, Mazzaferro V, et al. Sorafenib in advanced hepatocellular carcinoma. *The New England journal of medicine* 2008;359:378–90.
5. Cheng AL, Kang YK, Chen Z, et al. Efficacy and safety of sorafenib in patients in the Asia-Pacific region with advanced hepatocellular carcinoma: a phase III randomised, double-blind, placebo-controlled trial. *Lancet Oncol* 2009;10:25–34.
6. Villanueva A, Llovet JM. Second-line therapies in hepatocellular carcinoma: emergence of resistance to sorafenib. *Clin Cancer Res* 2012;18:1824–6.

7. Rudalska R, Dauch D, Longerich T, et al. In vivo RNAi screening identifies a mechanism of sorafenib resistance in liver cancer. *Nat Med* 2014;20:1138–46.
8. Chen KF, Chen HL, Tai WT, et al. Activation of phosphatidylinositol 3-kinase/Akt signaling pathway mediates acquired resistance to sorafenib in hepatocellular carcinoma cells. *J Pharmacol Exp Ther* 2011;337:155–61.
9. Fernando J, Malfettone A, Cepeda EB, et al. A mesenchymal-like phenotype and expression of CD44 predict lack of apoptotic response to sorafenib in liver tumor cells. *Int J Cancer* 2015;136:E161–72.
10. Fiume L, Manerba M, Vettraino M, Di Stefano G. Effect of sorafenib on the energy metabolism of hepatocellular carcinoma cells. *European journal of pharmacology* 2011;670:39–43.
11. Shen YC, Ou DL, Hsu C, et al. Activating oxidative phosphorylation by a pyruvate dehydrogenase kinase inhibitor overcomes sorafenib resistance of hepatocellular carcinoma. *Br J Cancer* 2013;108:72–81.
12. Tesori V, Piscaglia AC, Samengo D, et al. The multikinase inhibitor Sorafenib enhances glycolysis and

synergizes with glycolysis blockade for cancer cell killing. *Sci Rep* 2015;5:9149.

13. Reyes R, Wani NA, Ghoshal K, Jacob ST, Motiwala T. Sorafenib and 2-Deoxyglucose Synergistically Inhibit Proliferation of Both Sorafenib-Sensitive and -Resistant HCC Cells by Inhibiting ATP Production. *Gene Expr* 2017;17:129–40.

14. Gwak GY, Yoon JH, Kim KM, Lee HS, Chung JW, Gores GJ. Hypoxia stimulates proliferation of human hepatoma cells through the induction of hexokinase II expression. *Journal of hepatology* 2005;42:358–64.

15. Ihlund LS, Hernlund E, Khan O, Shoshan MC. 3-Bromopyruvate as inhibitor of tumour cell energy metabolism and chemopotentiator of platinum drugs. *Molecular oncology* 2008;2:94–101.

16. Gu HR, Park SC, Choi SJ, et al. Combined treatment with silibinin and either sorafenib or gefitinib enhances their growth-inhibiting effects in hepatocellular carcinoma cells. *Clinical and molecular hepatology* 2015;21:49–59.

17. Rahmani M, Davis EM, Crabtree TR, et al. The kinase inhibitor sorafenib induces cell death through a process

involving induction of endoplasmic reticulum stress. *Molecular and cellular biology* 2007;27:5499–513.

18. Holz MS, Janning A, Renne C, Gattenlohner S, Spieker T, Brauning A. Induction of endoplasmic reticulum stress by sorafenib and activation of NF- κ B by lestaurtinib as a novel resistance mechanism in Hodgkin lymphoma cell lines. *Molecular cancer therapeutics* 2013;12:173–83.

19. Yu SJ, Yoon JH, Yang JI, et al. Enhancement of hexokinase II inhibitor-induced apoptosis in hepatocellular carcinoma cells via augmenting ER stress and anti-angiogenesis by protein disulfide isomerase inhibition. *J Bioenerg Biomembr* 2012;44:101–15.

20. Yoo JJ, Lee DH, Cho Y, et al. Differential sensitivity of hepatocellular carcinoma cells to suppression of hepatocystin transcription under hypoxic conditions. *J Bioenerg Biomembr* 2016;48:581–90.

21. Carr BI, Wang Z, Wang M, Cavallini A, D'Alessandro R, Refolo MG. c-Met-Akt pathway-mediated enhancement of inhibitory c-Raf phosphorylation is involved in vitamin K1 and sorafenib synergy on HCC growth inhibition. *Cancer biology & therapy* 2011;12:531–8.

22. Shen Z, Wang X, Yu X, Zhang Y, Qin L. MMP16 promotes tumor metastasis and indicates poor prognosis in hepatocellular carcinoma. *Oncotarget* 2017;8:72197–204.
23. Riddle SR, Ahmad A, Ahmad S, et al. Hypoxia induces hexokinase II gene expression in human lung cell line A549. *American journal of physiology Lung cellular and molecular physiology* 2000;278:L407–16.
24. Park JG, Lee JH, Kang MS, et al. Characterization of cell lines established from human hepatocellular carcinoma. *International journal of cancer* 1995;62:276–82.
25. O'Connor R, Clynes M, Dowling P, O'Donovan N, O'Driscoll L. Drug resistance in cancer – searching for mechanisms, markers and therapeutic agents. *Expert opinion on drug metabolism & toxicology* 2007;3:805–17.
26. Zhai B, Sun XY. Mechanisms of resistance to sorafenib and the corresponding strategies in hepatocellular carcinoma. *World journal of hepatology* 2013;5:345–52.
27. Vander Heiden MG, Cantley LC, Thompson CB. Understanding the Warburg effect: the metabolic requirements of cell proliferation. *Science* 2009;324:1029–33.
28. Pelicano H, Martin DS, Xu RH, Huang P. Glycolysis

- inhibition for anticancer treatment. *Oncogene* 2006;25:4633–46.
29. Granchi C, Bertini S, Macchia M, Minutolo F. Inhibitors of lactate dehydrogenase isoforms and their therapeutic potentials. *Current medicinal chemistry* 2010;17:672–97.
30. Ganapathy–Kanniappan S, Geschwind JF, Kunjithapatham R, et al. 3–Bromopyruvate induces endoplasmic reticulum stress, overcomes autophagy and causes apoptosis in human HCC cell lines. *Anticancer research* 2010;30:923–35.
31. Can Z, Lele S, Zhirui Z, et al. 3–Bromopyruvate enhances TRAIL–induced apoptosis in human nasopharyngeal carcinoma cells through CHOP–dependent upregulation of TRAIL–R2. *Anti–cancer drugs* 2017;28:739–49.
32. Pedersen PL. 3–Bromopyruvate (3BP) a fast acting, promising, powerful, specific, and effective "small molecule" anti–cancer agent taken from labside to bedside: introduction to a special issue. *Journal of bioenergetics and biomembranes* 2012;44:1–6.
33. Kim W, Yoon JH, Jeong JM, et al. Apoptosis–inducing antitumor efficacy of hexokinase II inhibitor in hepatocellular carcinoma. *Molecular cancer therapeutics* 2007;6:2554–62.
34. Ko YH, Smith BL, Wang Y, et al. Advanced cancers:

eradication in all cases using 3-bromopyruvate therapy to deplete ATP. Biochemical and biophysical research communications 2004;324:269-75.

35. Geschwind JF, Ko YH, Torbenson MS, Magee C, Pedersen PL. Novel therapy for liver cancer: direct intraarterial injection of a potent inhibitor of ATP production. Cancer research 2002;62:3909-13.

36. Liang Y, Zheng T, Song R, et al. Hypoxia-mediated sorafenib resistance can be overcome by EF24 through Von Hippel-Lindau tumor suppressor-dependent HIF-1alpha inhibition in hepatocellular carcinoma. Hepatology 2013;57:1847-57.

37. Peng S, Wang Y, Peng H, et al. Autocrine vascular endothelial growth factor signaling promotes cell proliferation and modulates sorafenib treatment efficacy in hepatocellular carcinoma. Hepatology 2014;60:1264-77.

국문 초록

서론: 본 연구에서는 헥소키나아제-II 활성도의 저해가 *in-vivo* 모델의 간세포암에서 소라페닙의 효능을 증대시킬 수 있는지에 대해 알아보고, 다음으로 헥소키나아제-II 의 발현이 인간 간세포암에서 예후 인자로도 작용할 수 있는지 알아보고자 한다.

방법: 헥소키나아제-II 의 억제를 위해 3-브롬피루브산염을 사용하였다. 또한 인간 간세포암 세포주를 이용하여, BALB/c nu/nu 마우스에서 피하 및 동종 종양 이종 이식 실험을 시행하였다. 헥소키나아제-II 의 예후로서의 역할은 TCGA 데이터베이스의 간세포암 환자의 데이터를 이용하였고, 소라페닙을 사용한 환자의 데이터로 검증하였다.

결과: 정량적 실시간 PCR, 웨스턴 블롯 분석, 면역조직화학 염색을 통해 소라페닙을 투여할 경우 헥소키나아제-II 의 발현이 증가하는 것을 확인하였다. 두 개의 다른 마우스 간세포암 모델을 사용한 소포체-스트레스 모델에서 3-브롬피루브산염을 사용하여 추가적인 스트레스를 가할 경우, *in vivo* 와 *in vitro* 모두에서 소라페닙의 효능을 증가시키는 것을 확인하였다. 또한 TCGA 데이터 베이스에서 헥소키나아제-II 의 발현이 증가되어 있는 환자에서 전체 생존율이 낮았으며, 소라페닙 치료를 받은 TCGA 데이터베이스 간세포암 환자에서도 유사한 결과를 확인할 수 있었다.

결론: 헥소키나아제-II 는 소라페닙의 효능을 향상시키는 유망한 치료 표적이 될 수 있고, 또한 간세포암 환자에서 예후 인자로도 사용될 수 있다.

주요어: 간세포암, 소라페닙, 헥소키나아제 억제제, 브롬피루브산염학
번: 2015-30556